Bioorganic & Medicinal Chemistry 17 (2009) 1506–1513

Contents lists available at ScienceDirect

Bioorganic & Medicinal Chemistry

journal homepage: www.elsevier.com/locate/bmc

Novel *E. coli* β-ketoacyl-acyl carrier protein synthase III inhibitors as targeted antibiotics

Jee-Young Lee [a], Ki-Woong Jeong [a], Ju-Un Lee [a], Dong-Il Kang [b], Yangmee Kim [a,*]

[a] Department of Bioscience and Biotechnology, Bio/Molecular Informatics Center, Konkuk University, 1 Hwayang-dong, Kwangjin-gu, Seoul 143-701, Republic of Korea
[b] Department of Chemistry, Konkuk University, Seoul 143-701, Republic of Korea

ARTICLE INFO

Article history:
Received 11 November 2008
Revised 7 January 2009
Accepted 8 January 2009
Available online 11 January 2009

Keywords:
KAS
Antibiotics
In silico screening
STD-NMR

ABSTRACT

β-Ketoacyl-acyl carrier protein synthase (KAS) III is a condensing enzyme that initiates fatty acid biosynthesis in most bacteria. We determined three pharmacophore maps from receptor-oriented pharmacophore-based *in silico* screening of the X-ray structure of *Escherichia coli* KAS III (ecKAS III) and choose 16 compounds as candidate ecKAS III inhibitors. Binding inhibitors were characterized using saturation-transfer difference NMR spectroscopy (STD-NMR), and binding constants were determined with fluorescence quenching experiments. Based on the results, we propose that the antimicrobial compound, 4-cyclohexyliminomethyl-benzene-1,3-diol (YKAs3003), is a potent inhibitor of pathogenic KAS III, displaying minimal inhibitory concentration (MIC) values in the range 128–256 μg/mL against various bacteria.

1. Introduction

Fatty acids are an important source of energy for several organisms, and form a major component of all cell membranes. Fatty acid biosynthesis is a highly attractive molecular focus of drug discovery research. This biosynthetic pathway is the target of several classes of compounds displaying antimicrobial and antimalarial activities.[1,2]

Fatty acid synthesis, a common procedure in all organisms, is controlled by a multifunctional enzyme complex system (fatty acid synthase; FAS) with acetyl-CoA and malonyl-CoA as precursor substrates. FAS, a multienzyme complex system, consists of seven protein domains. Two basic types of FAS architecture exist in nature, designated FAS I and FAS II (reviewed by Rock).[1,3–5] While the two systems have distinct processes, the related enzymes are highly conserved. Remarkably, FAS I produces a single fatty acid, palmitate, while FAS II generates different products for cellular metabolism, including fatty acids of varying chain lengths.

FAS I has been identified in eukaryotic organisms, including animals and humans, and each reaction in this pathway is catalyzed by distinct domains of large multifunctional proteins.[6] Since the enzymatic activities are linked within a single polypeptide template with no intermediate diffusion from the complex, FAS I is considered a more efficient biosynthetic system.[3] FAS II participates in fatty acid biosynthesis in the majority of bacteria and plants. The FAS II enzyme system catalyzes the same type of reaction, but uses a series of monofunctional proteins that act on individual steps in the biosynthesis pathway.[5,7] This difference presents considerable potential for selective inhibition of the bacterial FAS systems.[8]

Fatty acid biosynthesis is initiated by the β-ketoacyl-acyl carrier protein synthase (KAS) protein.[6,9] The FAS II cycle promotes elongation of fatty acids through several reduction and dehydration steps. Among the related FAS II enzymes, the condensing protein, KAS, is an essential target for novel antibacterial drug design.[6,8] Three types of KAS (I, II, and III) have been identified to date. KAS I (encoded by *FabB*) and KAS II (*FabF*) are elongation condensing enzymes that use acyl-ACP as a primer to condense with malonyl-ACP.[5,8] The roles and structures of these two enzymes are similar, but a number of the important mechanisms differ from those of KAS III (encoded by *FabH*). KAS III catalyzes the initial condensation of acetyl-CoA with malonyl-ACP, and plays an essential role in bacterial fatty acid synthesis.[8,10] The initial condensation step of the FAS II system by KAS III is presented in Figure 1. The sequence homology between KAS I and KAS II is about 40%, while KAS III only displays overall homology of <10% with KAS I and KAS II.

KAS III, a 35–50 kDa protein with a homodimeric active form, acts as the condensing enzyme in various bacteria.[11] The active site contains a Cys-His-Asn catalytic triad, which is conserved in various bacterial KAS III molecules.[12–14] KAS III represents a promising target for the design of novel antimicrobial drugs, since this protein regulates the fatty acid biosynthesis rate via an initiation pathway and its substrate specificity is a key factor in membrane fatty acid composition.[15–17] Moreover, the three-dimensional structure of the protein is highly conserved in various bacteria, and its inhibitors may thus act as potent antibiotics with broad-spectrum activity.

* Corresponding author. Tel.: +82 2 450 3421; fax: +82 2 447 5987.
E-mail address: ymkim@konkuk.ac.kr (Y. Kim).

0968-0896/$ - see front matter © 2009 Elsevier Ltd. All rights reserved.
doi:10.1016/j.bmc.2009.01.004

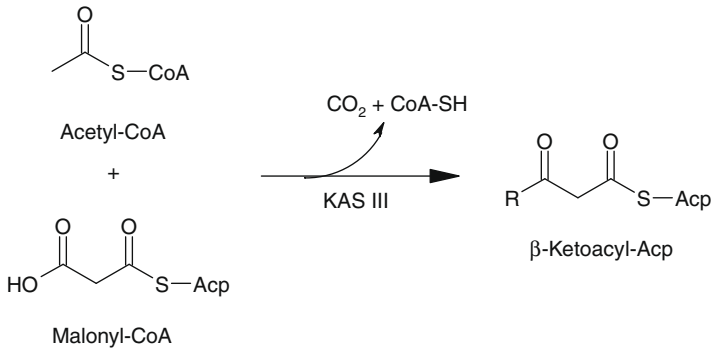

Figure 1. KAS III accomplishes the initial condensation step in FAS II.

Receptor-oriented pharmacophore-based *in silico* screening is an effective method to identify novel and specific ligands or inhibitors. Since the *in silico* screening process facilitates the systematic analysis of possible interactions between a large number of compounds and proteins with the detection of noncovalent interactions in protein active sites, it is an impact methodology of a rational drug design.[18–22] Analysis of protein active sites is important for establishing pharmacophore maps, and understanding receptor–ligand interactions is an essential step of *in silico* screening. Pharmacophore maps depict sets of interactions (chemical features or functionalities) aligned in three-dimensional space, and include several features, along with excluded volume regions based on receptor atom positions.[23,24] For each compound library, a multiple conformer database is constructed and searched with a set of pharmacophore maps. The resulting hits comprise various conformers of a subset of compounds that satisfy one or more maps, and are thus expected to fit the active site reasonably well.

In this study, we perform receptor-oriented pharmacophore-based *in silico* screening of *Escherichia coli* KAS III (ecKAS III), with the aim of identifying novel inhibitors. Candidate inhibitors displayed antimicrobial activity against Gram-negative *Escherichia coli* (*E. coli*) and *Klebsiella pneumonia* (*K. pneumonia*), Gram-positive *Staphylococcus aureus* (*S. aureus*) and *Enterococcus faecalis* (*E. faecalis*), *and Methicillin-resistant staphylococcus aureus* (MRSA), and were subsequently assessed for binding to ecKAS III using biophysical screening methods, such as STD-NMR and fluorescence quenching experiments.

2. Experimental

2.1. Receptor-oriented pharmacophore-based *in silico* screening

2.1.1. Building of a 3D compound database

250,000 Synthetic compounds from Specs.net (Kluyverweg, Netherlands) and Maybridge Chemical Company (Tintagel, Cornwall, England) included a database. All compounds were converted to 3D databases with multiple conformers by applying the catDB utility program, as implemented in Catalyst™ (Accelrys Inc., San Diego, CA).[25] Multiple conformers were generated using the FAST search method, and a maximum of 250 conformers was allowed within an energy cut-off range of 20 kcal/mol. Default values of all other parameters were applied.[25,26]

2.1.2. Receptor-oriented pharmacophore-based *in silico* screening of ecKAS III

Pharmacophores are typically defined by three chemical features, specifically, hydrogen bond donors (HBDs), hydrogen bond acceptors (HBAs) and lipophilicity (Lipo). Active sites of proteins or receptors often present these characteristics, which are combined to establish pharmacophore maps. Pharmacophore maps were determined with the excluded volume for heavy atoms, which is the forbidden area in the active site that defines its shape. An exclusion model was generated for the active site and surrounding receptor regions and heavy atoms in the receptor accounted for the excluded volume. Each receptor atom selected for inclusion in the model was presented as an exclusion point.[20–22]

We defined the active site of ecKAS III, based on the center and radius of the binding substrate in an X-ray structure of ecKAS III complexed with CoA or inhibitor.[27,28] Interaction models were generated within 10 Å of the active site center, and the features adjusted taking into account the substrate binding model. Among the multiple pharmacophore maps, the most favorable binding model of ecKAS III and substrate was established via test *in silico* screening with CoA. Pharmacophore maps that effectively expressed the binding model of enzyme with substrate were selected for searching the compound library. In this study, maps were determined with two groups. One group comprised three (two H-bond donor and one lipophilic feature) or four features (two H-bond donors, one acceptor, and one lipophilic feature) and the other was generated with two or three features and shape constraints. We selected the final inhibitor candidates from visual inspections and ligand score estimations (LigScore). These compounds were further subjected to antimicrobial and binding assays.

Computational studies were performed on a Linux environment using the Cerius^2/SBF module (Accelrys Inc., San Diego, CA) and catSearch utility, as implemented in Catalyst™ (Accelrys Inc., San Diego, CA).

2.2. Expression and purification of ecKAS III

2.2.1. Construction of the ecKAS III expression plasmid

The *fab*H gene encoding KAS III was amplified from *E. coli* K-12 genomic DNA. The sense primer, 5′-catatgtatacgaagattattggtact-3′, and antisense primer, 5′-ggatcctagaaacgaaccagcgcgg-3′, were designed on the basis of GenBank accession number 48994873. At the 5′ end of each primer, a restriction site (*Nde*I for the sense primer and *Bam*HI for the antisense primer) was attached to facilitate cloning. PCR was performed under the following conditions: 35 cycles of denaturation for 1 min at 94 °C, annealing for 1 min at 55 °C, and extension for 1 min at 72 °C. The resulting product was sequenced and cloned between the *Nde*I and *Bam*HI sites of pET-15b vector. The ligation mixture was transformed into *E. coli* DH5α competent cells.

2.2.2. Expression and purification of ecKAS III

The pET-15b/*ec*KAS III plasmid was transformed into the expression host, *E. coli* BL21 (DE3). Transformed cells were grown on Luria-

Bertani (LB) agar plates containing 50 μg/mL ampicillin. SDS-PAGE was employed to select a colony expressing *ec*KAS III with an N-terminal polyhistidine tag. One colony was used to inoculate 50 mL of LB medium with 50 μg/mL ampicillin, and grown overnight in a 37 °C shaking incubator. Fully grown culture (10 ml) was mixed with 1 l of fresh LB containing 50 μg/mL ampicillin, and grown at 37 °C until an optical density at 600 nm of 1.0. The culture was induced with 1 mM IPTG and grown for 5 more hours at 30 °C. Cells were harvested, and the pellet stored at −80 °C.

All lysis and purification procedures were performed at 4 °C. The frozen pellet was resuspended and lysed by ultrasonication in buffer A containing 50 mM sodium phosphate and 300 mM NaCl. The cell lysate was centrifuged and the supernatant loaded onto a HiTrap chelating column (GE) pre-equilibrated with buffer A. The column was washed with buffer A, and the bound material eluted with a linear gradient from 0 to 600 mM imidazole. The ecKAS III-containing fraction was pooled and concentrated with AmiconUltra (Millipore) using exchanging buffer B (50 mM sodium phosphate, 100 mM NaCl, pH 8.0). SDS-PAGE was applied to identify the ecKAS III-containing fraction at each stage of purification.

2.3. Binding assays

2.3.1. NMR screening

Saturation transfer difference NMR (STD-NMR) experiments were performed at 298 K.[29,30] The protein was saturated on-resonance at −1.0 ppm and off-resonance at 40 ppm, with a cascade of 40 selective Gaussian-shaped pulses of 50 ms duration and 100 μs delay between each pulse in all STD-NMR experiments. The total duration of the saturation time was set to 2 s.

For STD-NMR experiments, 10 μM recombinant ecKAS III in 50 mM sodium phosphate buffer, 100 mM NaCl, pH 8.0, and candidate inhibitors were mixed at a protein/ligand ratio of 1:100. In total, 1024 scans for each experiment were acquired, and a WATERGATE sequence used to suppress the water signal. A spin-lock filter (5 kHz strength and 10 ms duration) was applied to suppress the protein background. All NMR spectra were recorded on Varian Unity Plus 500 MHz and Bruker Avance 500 MHz NMR spectrometers at KBSI. Resonance assignments of ^{1}H NMR spectra of free ligands were completed using ^{1}H–^{1}H COSY, NOESY, HMBC, and HBQC experiments.

2.3.2. Fluorescence analysis

The binding constants of inhibitors and ecKAS III were measured on a model RF-5301PC spectrofluorophotometer (Shimadzu, Kyoto, Japan). The ecKAS III protein (10 μM) was added to buffer (50 mM sodium phosphate, 100 mM NaCl, pH 8.0). Each candidate inhibitor was titrated to a final protein/inhibitor ratio of 1:10. All solutions contained similar buffer concentrations. The sample was placed in a 2 mL thermostatted cuvette, with excitation and emission path lengths of 10 mm. Fluorescence quantum yields of ecKAS III and ligand were determined by tryptophan emission. Samples were excited at 290 nm, and emission spectra recorded for light scattering effects from 290 to 500 nm. We estimated the K_d value using Eq. 1:[31]

$$\log\left(\frac{F_0 - F}{F}\right) = \log\frac{1}{K_d} + n\log[\text{inhibitor}] \quad (1)$$

where F_0 and F represent fluorescence intensity from ecKAS III at 339 nm in the absence and presence of inhibitor, respectively, while n is the number of inhibitor binding sites on the protein.

2.3.3. The MIC test

The antimicrobial activities of inhibitor candidates were examined using the standard two-fold serial broth dilution method[32,33] with five bacterial species, including two Gram-negative bacteria (*E. coli* (KCTC 1682) and *K. pneumonia* (KCTC 2242)), three Gram-positive bacteria (*S. aureus* (KCTC 1621) and *E. faecalis* (KCTC 2011)), and MRSA (CCARM 3114). The four standard bacteria were purchased from the Korean Collection for Type Cultures (KCTC) (Taejon, Korea). The clinical isolate of MRSA (CCARM 3114) was supplied by Culture Collection of Antimicrobial Resistant Microbes (CCARM) (Seoul, Korea).

The bacterial suspension was adjusted to 0.5 McFarland standard prepared from a single colony on an agar plate incubated for 18–24 h, and diluted 10-fold in Mueller Hinton broth. A 20 μL aliquot of the diluted cell suspension (1×10^6 colony forming units) was used to inoculate each well of a 96-well plate containing 100 μL of the same medium with the indicated concentrations of candidate inhibitors. Plates were incubated at 37 °C for 20 h. MIC was defined as the lowest concentration of antibiotic leading to complete inhibition of visible growth in relation to an antibiotic-free control well. Experiments were replicated at least three times to verify methodology reproducibility using the above conditions.

3. Results and discussion

3.1. *In silico* screening of ecKAS III

In silico screening was performed on two binding models; Model 1 is based on the ecKAS III-CoA complex structure (1HNJ.pdb)[27] and model 2 on the ecKAS III-inhibitor complex structure (1MZS.pdb).[34] The 3D structure of ecKAS III is shown in Figure 2. The greatest difference between the two models is whether the substrate binds KAS III at the catalytic triad tunnel on the active site via polar or hydrophobic interactions. The KAS III active site generally contains a catalytic triad tunnel consisting of Cys-His-Asn, which is conserved in the majority of bacteria. This catalytic triad plays an important role in the regulation of chain elongation and substrate binding. Since the alkyl chain of CoA is broken by Cys of the catalytic triad of KAS III, interactions between Cys and substrate appear to play an important role in substrate binding. Qiu group (Qiu, X. et al., 2001) have been refined three-dimensional structure of ecKAS III in the presence and absence of malonyl-CoA by X-ray spectroscopy. Since malonyl moiety is degraded by ecKAS III, molecular docking studies for KAS III and malonyl-CoA was carried out to identify a plausible malonyl-binding mode.[27] They found that in one of the binding modes appeared in the lower scored conformations, the malonyl carboxylate formed hydrogen bonds to the backbone nitrogen of Phe304. Based on this report, we designed pharmacophore maps considering the interaction with Phe304. Phe304 located in the vicinity of the free terminal thiol group of CoA, and that malonyl carbonyl oxygen is located near the side-chains of His244 and Asn274, but does not form hydrogen bonds with His244 and Asn274 residues.[27] In the X-ray structure of ecKAS III complexed with an indole inhibitor, a dichlorobenzyl ring (a hydrophobic functional group of the inhibitor) occupies the catalytic triad tunnel instead of a polar group.[34]

The geometric center of the ecKAS III substrate was used to define the active site center. The 9.0 Å radius includes all the residues forming the first shell around CoA or inhibitor bound to the receptor. Chemical features were generated from receptor atoms within 9.0 Å from the active site center.

Consequently, we established three pharmacophore maps (I, II and III). Maps I and II belong to model 1, while Map III is related to model 2. Pharmacophore maps were generated from the interaction and exclusion models, using all possible combinations of the three or four features. To prioritize and select optimal pharmacophore maps, we performed self-hit test with multiple conformer database of malonyl-CoA. In our self-hit-test, we prioritized the

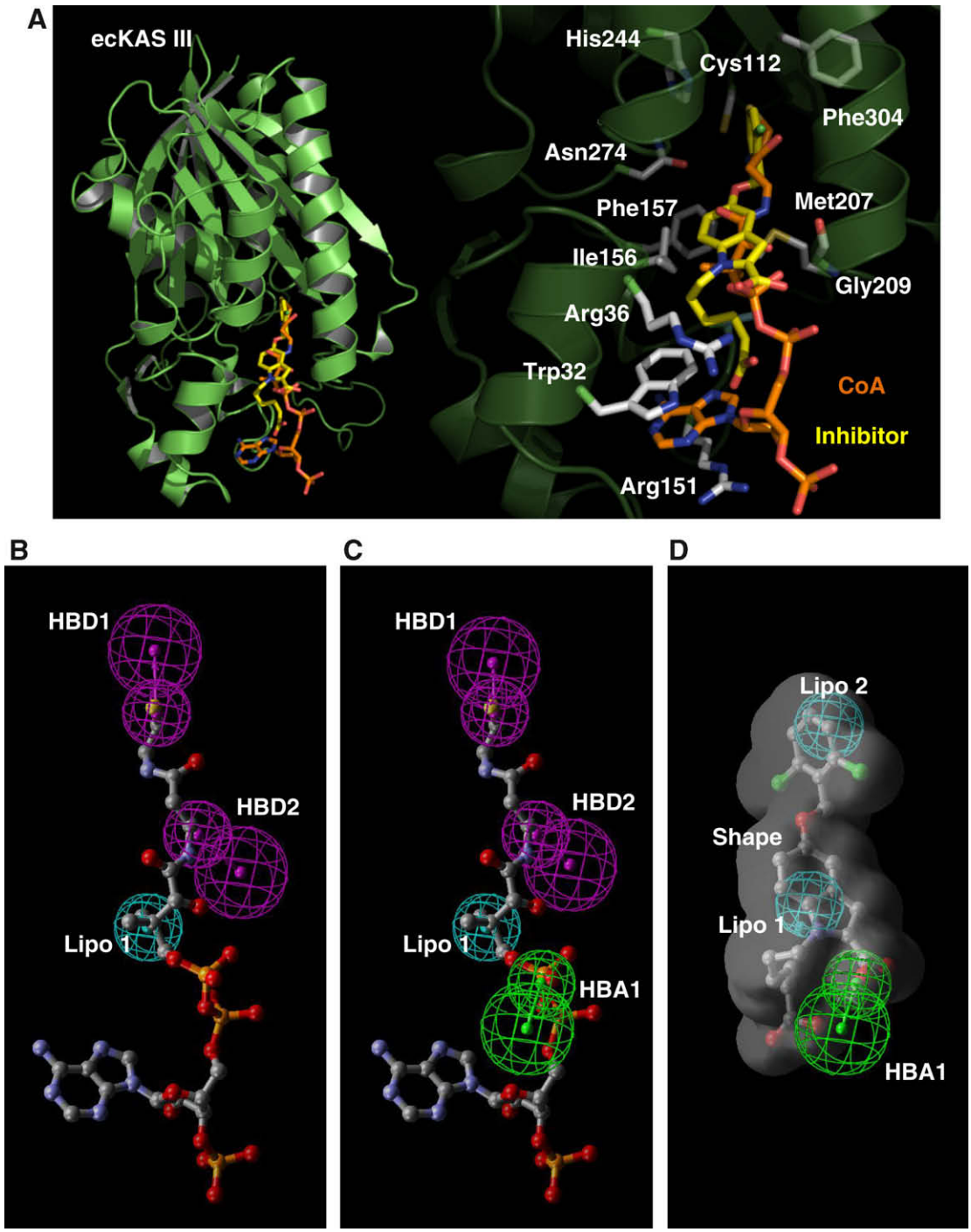

Figure 2. 3D Structure of ecKAS III and pharmacophore maps determined using receptor-oriented pharmacophore-based *in silico* screening. (A) Structure of ecKAS III and its binding site, (B) Pharmacophore Map I, (C) Map II, and (D) Map III.

maps that reproduced the coordination of substrate and the binding model of CoA-KAS III at the X-ray structure most similarly (rmsd < 0.4 Å). Then, the maps were utilized to screen large databases. Among the 12 pharmacophore maps generated, only two (Maps I and II) effectively represented the binding model of CoA-KAS III. Map I consisted of three features, specifically, two hydrogen bond donors (HBD1 and HBD2) that involving the backbone oxygen of Phe304 and Gly209, respectively, and one hydrophobic interaction (Lipo1) with Ile156, Phe157 and Met207. Map II comprised four features, specifically, two HBD (HBD1 and HBD2), a hydrogen bond acceptor (HBA1, representing a hydrogen bond with the Arg36 side-chain), and one hydrophobic interaction (Lipo1) common to both maps.

Model 2 represents interactions between ecKAS III and a known inhibitor, 1-(5-carboxy-pentyl)-5-(2,6-dichlorobenzyloxy)-1*H*-indole-2-carboxylic acid. In this model, hydrophobic interactions at the catalytic triad tunnel are important, and the inhibitor forms hydrogen bonds specifically with Arg36 and Arg151 of KAS III. Pharmacophore maps were determined by considering the interactions between these two residues. The hydrophobic interaction was formed with several specified residues of the active site pocket (Phe157, Ile156, Leu189, and Met207). Map III involved three fea-

tures, specifically, one hydrogen acceptor (HBA1, representing a hydrogen bond with a side-chain of Arg36) and two lipo features (Lipo1 and 2). A shape constraint was applied to regulate the number of compounds.[35] We also performed self-hit test with multiple conformer database of known inhibitor, 1-(5-carboxy-pentyl)-5-(2,6-dichlorobenzyloxy)-1*H*-indole-2-carboxylic acid, and confirmed that among six pharmacophore maps, only Map III reproduced the binding model of inhibitor-KAS III similar to the X-ray structure within 0.1 Å rmsd.

The three maps were used to search a database built with 250,000 compounds and 1074 compounds were hit by three maps. We initially selected 100 potential candidate ecKAS III inhibitors, based on ligand scores (LigScore) range from 5.70 to 3.67.[36,37] Finally, 16 candidates were selected by visual inspection considering the structural novelty of compounds. The two-dimensional structures of the selected compounds are depicted in Figure 3. These compounds were further subjected to medium-throughput screening.

3.2. Binding assay using NMR spectroscopy and fluorescence experiments

The difference spectra of candidates obtained from STD-NMR experiments disclosed resonances belonging to ligand protons bound to ecKAS III. Among 16 candidates, 8 compounds bind to ecKAS III. Our experiments additionally confirmed that the reference molecule, thiolactomycin (TLM), a known antibiotic inhibitor of ecKAS III, interacted with the enzyme, as expected.[38–40] STD-NMR spectra of TLM and YKAs3003 are shown in Figure 4.

When small molecules bind a comparably large protein, magnetization is transferred from protons of the protein to spatially close protons of the ligand.[41,42] The transferred magnetization can be measured after ligand dissociation from the protein.[42,43] Binding constants of these 8 compounds and TLM were determined using fluorescence quenching experiments. The ecKAS III protein contains six Trp residues at positions 56, 113, 123, 140, 221, and 276. Trp221 is in close proximity to the binding site. Protein fluorescence was visibly decreased upon binding of inhibitors. This quenching of fluorescence was used to estimate the binding constant. The binding (or dissociation) constant, K_d, is defined as [free protein] [free inhibitor]/[complex].[44] Fluorescence titration curves of compounds are presented in Figure 5. The fluorescence intensity was altered with increasing inhibitor concentrations. These changes were attributed to the formation of a protein–inhibitor complex. The K_d values of the strong binding inhibitors, YKAs3003 and YKA3013, were estimated as 0.02 and 1.22 μM, respectively, while that of the known inhibitor, TLM, was 121 μM. YKAs3003 was hit by Map I and YKA3013 by Map III. The binding affinities and results of STD-NMR are listed in Table 1. Based on these results, we suggest that the strongly binding compounds, YKAs3003 and YKA3013, are potent inhibitors of ecKAS III.

3.3. Antimicrobial activities of ecKAS III inhibitors

To establish the antimicrobial activities of the 8 candidate compounds, we measured their minimal inhibitory concentration (MIC) values against *E. coli*, *K. pneumonia*, *S. aureus*, *E. faecalis* and MRSA. Two compounds (YKAs3001 and YKAs3003) displayed antibacterial activity within a range of 128–256 μg/mL. YKAs3003 exhibited broad-spectrum activity against all bacterial strains. The MIC value of YKAs3003 against gram-negative *E. coli* and *K. pneumonia* was estimated as 128 μg/mL. For gram-positive bacteria, such as *S. aureus* and *E. faecalis*, the MIC value of YKAs3003 was 256 μg/mL. These values are similar to the MIC values

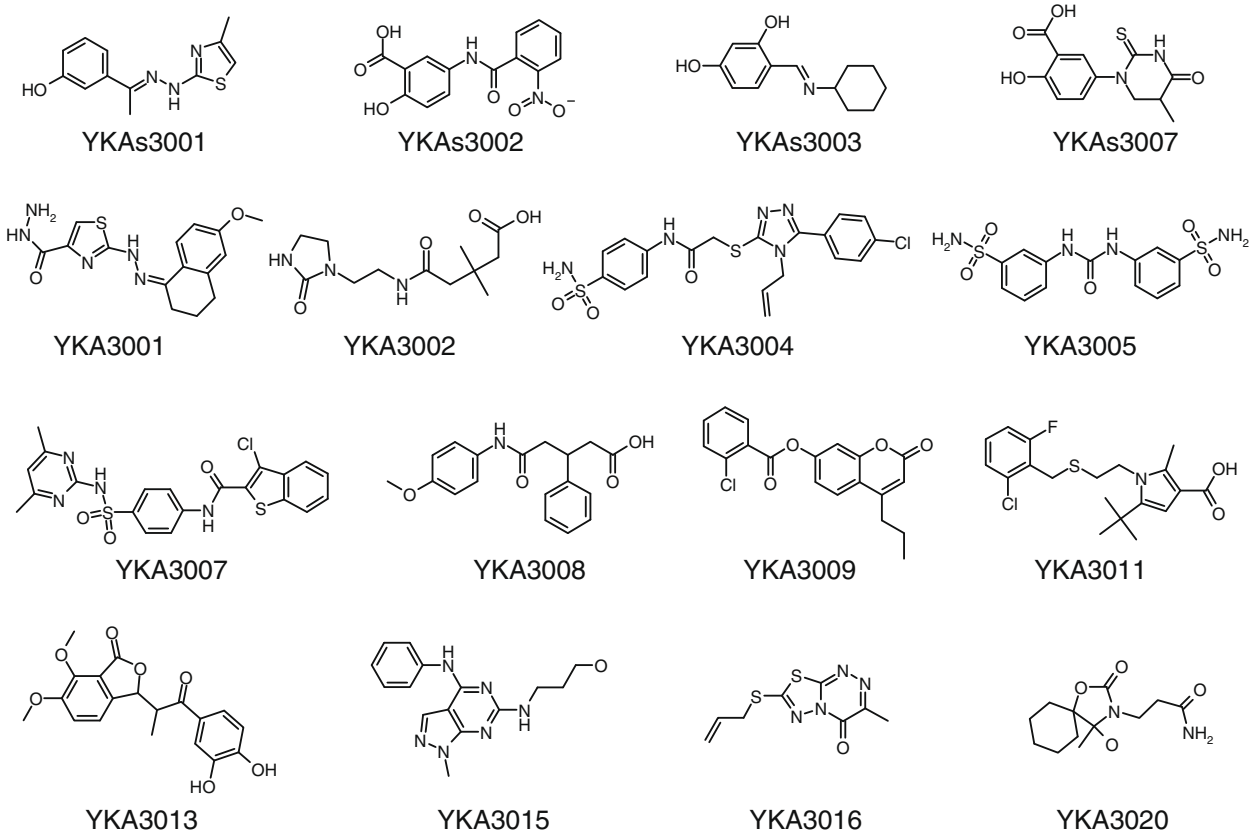

Figure 3. 2D Structures of selected compounds hit by receptor-oriented pharmacophore-based *in silico* screening.

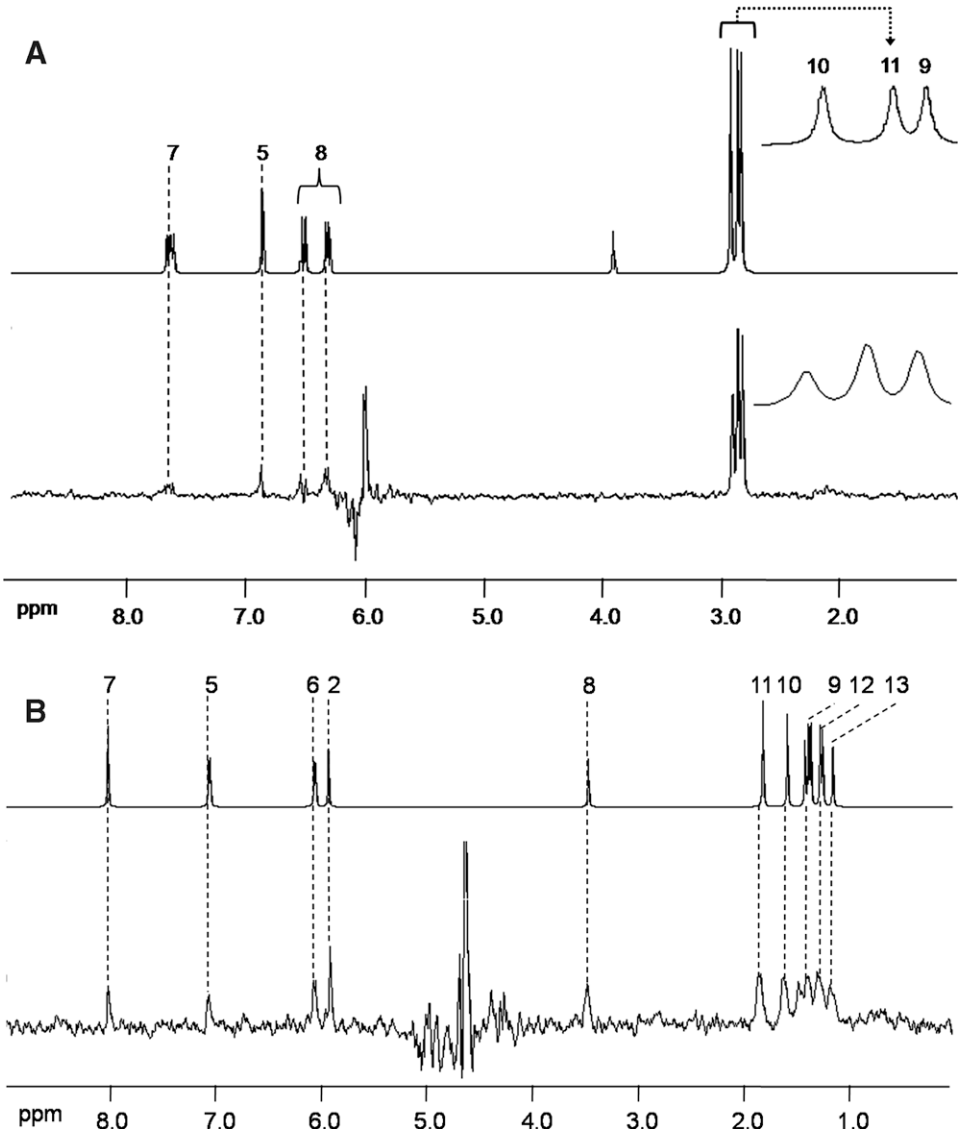

Figure 4. Representative results of the STD-NMR binding assay. (A) TLM and (B) YKAs3003.

obtained with TLM.[39] YKAs3001 did not display activity against gram-negative bacteria. We propose that the outer membrane of gram-negative bacteria acts as a barrier for this compound.[45,46] All three compounds displayed antimicrobial activity against MRSA. Notably, the MIC activity of YKAs3001 was lower than those of TLM and YKAs3003. The antimicrobial activities of these compounds are listed in Table 2. Based on these results, we propose that YAKs3003 is an inhibitor of ecKAS III with broad-spectrum antimicrobial activity.

While YKAs3001 displayed similar antimicrobial activity to YKAs3003, its low binding affinity implies that this compound does not inhibit ecKAS III, but acts on other target proteins. YKA3013 did not show antimicrobial activity but was a strong binding compound. It may be due to difficulty in penetrating the bacterial cell wall of YKA3013.

To estimate the cell permeability of YKA3013, we calculated *c*Log*P* and topological polar surface area (TPSA) for four compounds as listed in Table 2. *c*Log*P* is the partition coefficient between water and octanol as a factor of the lipophilicity of molecules.[47,48] PSA is defined as the surface sum over all polar atoms, in particular, TPSA is based on the summation of tabulated surface contributions of polar fragments.[49] These two properties are commonly used functions for the determination of cell permeability in transport across membranes.[49–51] We used software of Molinspiration (http://www.molinspiration.com) for calculations of *c*Log*P* and TPSA.[49] In Table 2, *c*Log*P* of YKA3013 is smaller than those of YKAs3003 and TLM, and similar to that of YKAs3001. Therefore, the lipophilicity of YKA3013 is smaller than those of YKAs3003 and TLM. TPSA of YKA3013 is about 2-fold larger than those of the rest three compounds. The low lipophilicity and large TPSA are known as the common causes of poor cell permeability. Based on calculated *c*LogP and PSA, we can conclude that YKA3013 has more difficulty to permeate the cell membrane compared with YKAs3001 and TLM.

The antibiotic activity of YKA3013 may be optimized by solving the problems related to its penetration of the cell membrane.

3.4. Binding model of YKAs3003 and ecKAS III

STD-NMR may be applied to analyze site-specific binding of ligands, since the chemical moiety of the ligand in strongest contact with protein displays the most intense NMR signals.[29,52–55] STD-NMR has been utilized for mapping binding epitopes of ligand.[47–51] The largest STD signal in each compound was set to 100%, and

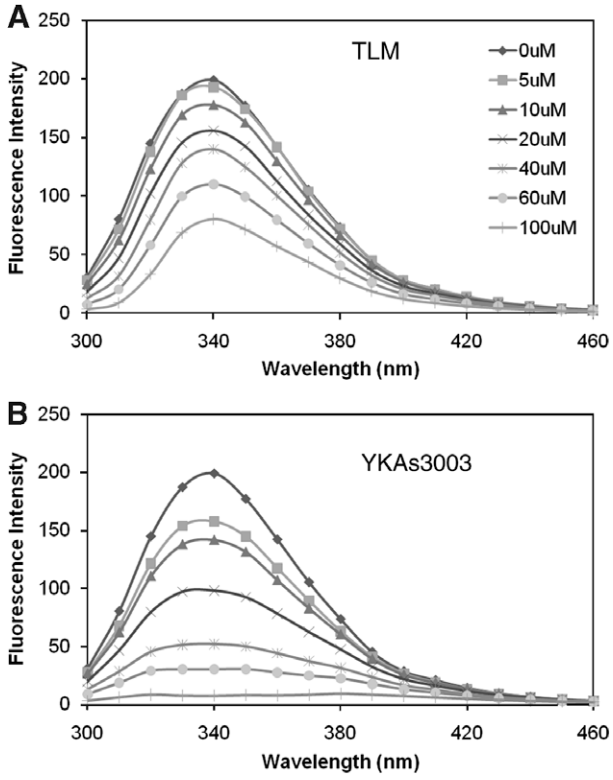

Figure 5. Fluorescence spectra of 0–100 μM. (A) TLM and (B) YKAs3003.

the relative intensities determined, as common for non-refined STD effects.[52] As reported in the group epitope mapping analysis, relative intensities were calculated according to Eq. 2 by comparing the intensities of signals in the STD-NMR spectrum (I_{STD}) with that of a reference spectrum (I_0).[29]

$$A_{STD} = \frac{(I_0 - I_{sat})}{I_0} = \frac{I_{STD}}{I_0} \quad (2)$$

Figure 6 presents the relative intensity of saturation for individual protons of TLM and YKAs3003. In TLM, methyl protons of C11 were assigned the highest intensity value of 100%, signifying very close contact with ecKAS III protein upon binding. Protons of C9 and C8 were awarded values of 87% and 90%, respectively. These moieties contribute to hydrophobic interactions with the protein.

The chemical designation of YKAs3003 is 4-cyclohexyliminomethyl-benzene-1,3-diol. The compound contains benzene-1,3-diol

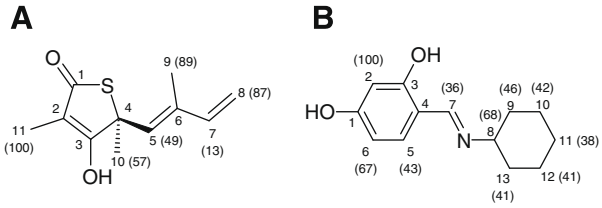

Figure 6. 2D structures of (A) TLM and (B) YKAs3003, and the relative degree (%) of saturation of individual protons determined from 1D STD-NMR spectra.

Table 1
STD-NMR and fluorescence quenching experiments

Pharmacophore maps	Compounds	Binding assay by STD-NMR	K_d (μM)
—	TLM	Binding	121
Map I	YKAs3001	Binding	>1000
	YKAs3002	Binding	>1000
	YKAs3003	Binding	0.02
	YKAs3007	Binding	>1000
Map II	YKA3001	Non-binding	—[a]
	YKA3002	Binding	>1000
	YKA3004	Non-binding	—
	YKA3005	Non-binding	—
Map III	YKA3007	Non-binding	—
	YKA3008	Non-binding	—
	YKA3009	Non-binding	—
	YKA3011	Non-binding	—
	YKA3013	Binding	1.22
	YKA3015	Binding	141
	YKA3016	Binding	>1000
	YKA3020	Non-binding	—

K_d is presented in μm.
[a] STD screening shows that these compounds do not bind ecKAS III. Fluorescence quenching experiments were only performed for compounds that bound to ecKAS III.

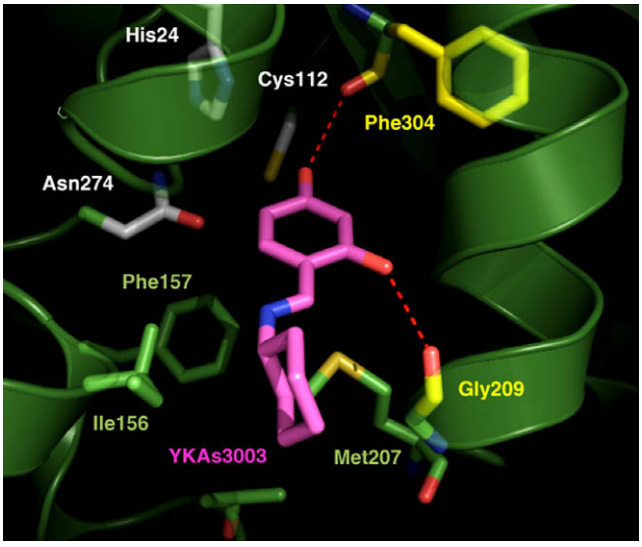

Figure 7. Binding model of YKAs3003 and ecKAS III hit by Map I. The catalytic triad is colored white, hydrophobic residues are green, and residues that participate in hydrogen bonding with YKAs3003 are yellow.

Table 2
MIC (μg/mL) values of four compounds, TLM, YKAs3001, YKAs3003, and YKA3013 against *E. coli, K. pneumonia, S. aureus, E. faecalis,* and MRSA, and calculated molecular properties of compounds

Compound	Gram-negative		Gram-positive			*C*Log*P*[a]	TPSA[b]
	E. coli	*K. pneumoniae*	*S. aureus*	*E. faecalis*	MRSA		
TLM	128	256	256	256	128	3.01	37.30
YKAs3001	>1024	>1024	256	256	256	2.45	57.51
YKAs3003	128	256	256	256	128	3.12	52.82
YKA3013	>1024	>1024	>1024	>1024	>1024	2.29	102.3

[a] *C*Log*P* is calculated using software of Molinspiration (www.molinspiration.com).[49,50]
[b] Topology polar surface area (TPSA) is calculated using software of Molinspiration (www.molinspiration.com).[49,50]

and a cyclohexane moiety, which are connected with a methyl imino group. The proton of C2 was assigned the highest intensity (100%), while the relative intensity of the proton of C6 was 66%. C2 is located between two hydroxy groups (HO1 and HO3), and C6 is close to HO1. The two hydroxy groups in YKAs3003 were not detected in the ^{1}H NMR spectrum. Since the resonances of ligand protons that are chemically exchangeable with protons of the solvent do not appear, they are not detected by STD-NMR upon binding.[42] Therefore, the benzene-1,3-diol moiety exhibiting a high degree of saturation is strongly recognized by ecKAS III, and may be critical for binding affinity. The proton of C8 displayed strong intensity (68%), compared to the rest of the protons on cyclohexane, with a STD effect in the range of 38–59%. It is proposed that this moiety interacts with the protein predominantly through the C8 region. In a hit model of YKAs3003, C8 is close to Ile156, and may participate primarily in hydrophobic interactions, compared to the other atoms in cyclohexane.

YKAs3003 was hit by pharmacophore map I consisting of three features (HBD1 and HBD2 depicting the backbone carbonyl oxygens of Phe304 and Gly209, respectively, and one hydrophobic interaction (Lipo1) with Ile156, Phe157 and Met207). In the hit model, HO1 and HO3 form hydrogen bonds with backbone carboxyl oxygens of Phe304 and Gly209, respectively. Cyclohexane may form a hydrophobic interaction with Ile156, Phe157 and Met207 of ecKAS III. The binding model of YKAs3003 and ecKAS III is depicted in Figure 7. Our STD results correlate well with the known binding models of YKAs3003 and ecKAS III determined from *in silico* screening. The binding information obtained from STD-NMR should facilitate the optimization of hit compounds and identification of novel structural compounds via *in silico* screening.

We propose that YKAs3003 is a potent inhibitor of *ec*KAS III with antimicrobial activity, and *in silico* screening data provide sufficient information to design effective ecKAS III inhibitors. Further optimization of this compound is required to improve its antimicrobial activity.

Acknowledgements

This work was supported by the Research Program for New Drug Target Discovery Grant (M10301030001-05N0103-00110) from the Ministry of Science and Technology. Ki-Woong Jeong was supported, in part, by the second BK21 (MOE). We thank professor Joong-Hoon Ahn at Konkuk University for helpful discussion.

References and notes

1. Heath, R. J.; White, S. W.; Rock, C. O. *Prog. Lipid Res.* **2001**, *40*, 467.
2. Lu, J. Z.; Lee, P. J.; Waters, N. C.; Prigge, S. T. *Comb. Chem. High Throughput Screening* **2005**, *8*, 15.
3. Lu, Y. J.; Zhang, Y. M.; Rock, C. O. *Biochem. Cell Biol.* **2004**, *82*, 145.
4. Marrakchi, H.; Zhang, Y. M.; Rock, C. O. *Biochem. Soc. Trans.* **2002**, *30*, 1050.
5. White, S. W.; Zheng, J.; Zhang, Y. M.; Rock, C. O. *Annu. Rev. Biochem.* **2005**, *74*, 791.
6. Lai, C. Y.; Cronan, J. E. *J. Biol. Chem.* **2003**, *19*, 51494.
7. Veyron-Churlet, R.; Guerrini, O.; Mourey, L.; Daffé, M.; Zerbib, D. *Mol. Microbiol.* **2004**, *54*, 1161.
8. Khandekar, S. S.; Daines, R. A.; Lonsdale, J. T. *Curr. Protein Pept. Sci.* **2003**, *4*, 21.
9. Heath, R. J.; Rock, C. O. *J. Biol. Chem.* **1996**, *3*, 10996.
10. Heath, R. J.; Rock, C. O. *Nat. Prod. Rep.* **2002**, *19*, 581.
11. Tsay, J. T.; Oh, W.; Larson, T. J.; Jackowski, S.; Rock, C. O. *J. Biol. Chem.* **1992**, *267*, 6807.
12. Christensen, C. E.; Kragelund, B. B.; von Wettstein-Knowles, P.; Henriksen, A. *Protein Sci.* **2007**, *16*, 261.
13. Bylka, W.; Matlawska, I.; Pilewski, N. A. *JANA* **2004**, *7*, 24.
14. Huycke, M. M.; Sahm, D. F.; Gilmore, M. S. *Emergen. Infect. Dis.* **1998**, *4*, 239.
15. Puupponen-Pimiä, R.; Nohynek, L.; Meier, C.; Kähkönen, M.; Heinonen, A. H. *J. Appl. Microbiol.* **2001**, *90*, 494.
16. Qiu, X.; Janson, C. A.; Konstantinidis, A. K.; Nwagwu, S.; Silverman, C.; Smith, W. W.; Khandekar, S.; Lonsdale, J.; Abdel-Meguid, S. S. *J. Biol. Chem.* **1999**, *274*, 36465.
17. Vladimir, B.; Nikolai, P. *Exp. Rev. Clin. Immunol.* **2005**, *1*, 145.
18. McInnes, C. *Curr. Opin. Chem. Biol.* **2007**, *11*, 494.
19. Kirchmair, J.; Ristic, S.; Eder, K.; Markt, P.; Wolber, G.; Laggner, C.; Langer, T. *J. Chem. Inf. Modell.* **2007**, *47*, 2182.
20. Hoffrén, A. M.; Murray, C. M.; Hoffmann, R. D. *Curr. Pharm. Des.* **2001**, *7*, 547.
21. Fisher, L. S.; Güner, O. F. *J. Braz. Chem. Soc.* **2002**, *13*, 777.
22. Kirchhoff, P. D.; Brown, R.; Kahn, S.; Waldman, M.; Venkatachalam, C. M. *J. Comput. Chem.* **2001**, *22*, 993.
23. Pickett, S. D.; Mason, J. S.; McLay, I. M. *J. Chem. Inf. Comput. Sci.* **1996**, *36*, 1214.
24. Elhallaoui, M.; Laguerre, M.; Carpy, A.; Ouazzani, F. C. *J. Mol. Model.* **2002**, *8*, 65.
25. CATALYST Version 4.10 software, **2000**, Accelrys Inc., San Diego, CA.
26. Murrall, N. W.; Davies, E. K. *J. Chem. Inf. Comput. Sci.* **1990**, *30*, 312.
27. Qiu, X.; Janson, C. A.; Smith, W. W.; Head, M.; Lonsdale, J.; Konstantinidis, A. K. *J. Mol. Biol.* **2001**, *307*, 341.
28. Alhamadsheh, M. M.; Musayev, F.; Komissarov, A. A.; Sachdeva, S.; Wright, H. T.; Scarsdale, N.; Florova, G.; Reynolds, K. A. *Chem. Biol.* **2007**, *14*, 513.
29. Mayer, M.; Meyer, B. *J. Am. Chem. Soc.* **2001**, *123*, 6108.
30. Macnaughtan, M. A.; Kamar, M.; Alvarez-Manilla, G.; Venot, A.; Glushka, J.; Pierce, J. M.; Prestegard, J. H. *J. Mol. Biol.* **2006**, *366*, 1266.
31. Mishra, B.; Barik, A.; Priyadarsini, K. I.; Mohan, H. *J. Chem. Sci.* **2005**, *117*, 641.
32. MacLowry, J. D.; Jaqua, M. J.; Selepak, S. T. *Appl. Microbiol.* **1970**, *20*, 46.
33. Smaill, F. *Can. J. Gastroenterol.* **2000**, *14*, 871.
34. Daines, R. A.; Pendrak, I.; Sham, K.; Van Aller, G. S.; Konstantinidis, A. K.; Lonsdale, J. T.; Janson, C. A.; Qiu, X.; Brandt, M.; Khandekar, S. S.; Silverman, C.; Head, M. S. *J. Med. Chem.* **2003**, *46*, 5.
35. Mason, J. S.; Beno, B. R. *J. Mol. Graphics Modell.* **2000**, *18*, 438.
36. Venkatachalam, C. M.; Jiang, X.; Oldfield, T.; Waldman, M. *J. Mol. Graphics Modell.* **2003**, *21*, 289.
37. Aparna, V.; Rambabu, G.; Panigrahi, S. K.; Sarma, J. A.; Desiraju, G. R. *J. Chem. Inf. Model.* **2005**, *45*, 725.
38. Price, A. C.; Choi, K. H.; Heath, R. J.; Li, Z.; White, S. W.; Rock, C. O. *J. Biol. Chem.* **2001**, *276*, 6551.
39. Noto, T.; Miyakawa, S.; Oishi, H.; Endo, H.; Okazaki, H. *J. Antibiot. (Tokyo).* **1982**, *35*, 401.
40. Heath, R. J.; Rock, C. O. *Curr. Opin. Invest. Drugs.* **2004**, *5*, 146.
41. Krishna, N. R.; Jayalakshmi, V. *Prog. Nucl. Magn. Reson. Spectrosc.* **2006**, *49*, 1.
42. Brecker, L.; Straganz, G. D.; Tyl, C. E.; Steiner, W.; Nidetzky, B. *J. Mol. Catal. B: Enzym.* **2006**, *42*, 85.
43. Meyer, B.; Peters, T. *Angew. Chem., Int. Ed.* **2003**, *42*, 864.
44. Möller, M.; Denicola, A. *Biochem. Mol. Biol. Educ.* **2002**, *30*, 309.
45. Nakae, T. *Crit. Rev. Microbiol.* **1986**, *13*, 1.
46. Vaara, M. *J. Antimicrob. Chemother.* **1992**, *29*, 221.
47. Jensen, B. F.; Refsgaardb, H. H. F.; Broc, R.; Brockhoff, P. B. *QSAR Comb. Sci.* **2005**, *24*, 449.
48. Veber, D. F.; Johnson, S. R.; Cheng, H. Y.; Smith, B. R.; Ward, K. W.; Kopple, K. D. *J. Med. Chem.* **2002**, *45*, 2615.
49. Ertl, P.; Rohde, B.; Selzer, P. *J. Med. Chem.* **2000**, *43*, 3714.
50. Wiemer, A. J.; Yu, J. S.; Shull, L. W.; Barney, R. J.; Wasko, B. M.; Lamb, K. M.; Hohl, R. J.; Wiemer, D. F. *Bioorg. Med. Chem.* **2008**, *16*, 3652.
51. Irwin, J. J.; Shoichet, B. K. *J. Chem. Inf. Model.* **2005**, *45*, 177.
52. Brecker, L.; Straganz, G. D.; Tyl, C. E.; Steiner, W.; Nidetzky, B. *J. Mol. Catal. B: Enzym.* **2006**, *42*, 85.
53. Haselhorst, T.; Blanchard, H.; Frank, M.; Kraschnefski, M. J.; Kiefel, M. J.; Szyczew, A. J.; Dyason, J. C.; Fleming, F.; Holloway, G.; Coulson, B. S.; Von Itzstein, M. *Glycobiology* **2007**, *17*, 68–81.
54. Nissler, L.; Gebhardt, R.; Berger, S. *Anal. Bioanal. Chem.* **2004**, *379*, 1045.
55. Johnson, M. A.; Pinto, B. M. *Bioorg. Med. Chem.* **2004**, *12*, 295.